



# Thermal Stress Effect on Fracture Integrity in Enhanced Geothermal Systems

Chao Zeng, Wen Deng<sup>(✉)</sup>, Chenglin Wu, and Matt Insall

Missouri University of Science and Technology, Rolla, MO 65401, USA  
wendeng@mst.edu

**Abstract.** In an enhanced geothermal system (EGS), fluid is injected into pre-existing fractures to be heated up and then pumped out for the electricity generation; injected fluid is cold as compared to surrounding bedrock. The rock-fluid temperature difference induces thermal stress along the fracture wall, and the large thermal stress could damage some of the self-propping asperities and result in a change of the topography and lifespan of the fractures. Although fracture sustainability has been extensively studied, the mechanism of asperity damage due to rock-fluid temperature difference remains unknown. We have constructed a finite-element based three-dimensional model, which uses a hemisphere contact pair to resemble a single self-propping asperity, to investigate the effect of temperature difference on the asperity damage. In the model, the rock mechanical properties are coupled with temperature and stress state of the bedrock. Two trends of asperity deformation with temperature effect are identified: opening zone and closure zone. Closure squeezes asperity further and induces more element damage at bottom. Higher temperature difference damages elements on asperity top whereas has negligible impact on elements at asperity bottom. In other aspect, a higher temperature expands closure zone and degrades elements at the asperity bottom. Accordingly, two potential mechanisms of asperity damage are qualitatively characterized.

**Keywords:** Fracture integrity · Thermal effect · Asperity failure

## 1 Introduction

Enhanced geothermal systems (EGS) offer a promising clean-energy resource in the world with enormous potential for baseload electricity generation [1, 2]. Unlike hydrothermal energy in shallow soil, EGS uses hot dry rock in deep earth formation: at depths of approximately 3 km to 10 km, and temperatures of up to 200 °C, the rock formations are ripe for energy extraction. An EGS injects cold water into such an environment and the heated water is brought back to the earth surface in the form of water vapor for electricity generation. In the EGS, the pre-existing fracture networks inside the hot rock play a crucial role, providing fluid (liquid water and steam) transport conduits and interfaces for heat exchange. The pre-existing fractures sustain themselves by propping due to asperities provided by contact roughness, which is different from corresponding mechanisms in the hydraulic fracture industry, which involve proppants that help maintain fracture integrity. The topography of fractures in EGS significantly

influences the geothermal energy extraction. Guo et al. [3] developed a thermos-hydro-mechanical coupled numerical model to analyze the effect of fracture aperture distribution on flow pattern evolution and temperature propagation. In their work, a generic fracture aperture of fracture was represented by a spatially spherical variogram model to consider the roughness effect. They observed that a reservoir tends to degrade flow channeling and endure heat production if the initial aperture field enables tortuous flow paths. Through a fracture with initially specified tortuosity, thermally-induced stress shrinks the rock matrix in cooled zones and deteriorates flow channeling, and accordingly shortens heat production life in contrast to its counterpart (which includes no consideration of thermal stress). Luo et al. [4] also pointed out that the distribution of fracture surface roughness, which is widely used to calculate fracture transmissivity, is of central importance to mechanical-hydraulic aperture correlations, because it leads to flow channeling and a steep temperature breakthrough curve.

When cold water is pumped into these fractures, the large temperature difference between rock and water induces extremely large tensile thermal stress which could deform the rock matrix. Pandey et al. [5] specifically analyzed the extent to which the thermos-elastic effect alters aperture. The cooling of the reservoir could cause contraction of the rock matrix and result in enlargement of fracture aperture in the vicinity of the injection well and conversely depresses regions outside of cooling zones. In light of increased aperture in direction between injection well and production wells, cold water directly flows from injection well to production well with least resistance and enables flow channeling and rapid drop in production temperature. Furthermore, the evolution of aperture field could reduce fluid pressure significantly in the long term, which influence aperture alteration in turn. Field circulation tests in enhanced fractured geothermal pilot program i.e. Soultz-sous-Forêts validated the occurrence of thermal contraction zone and temperature evolution [6]. In other aspect, the influence of thermal processes on new fracture opening had been addressed. Tarasovs et al. [7] studied the thermally-induced tensile cracking on primary fracture surface. The existing dominant fracture was simplified as half-plane surface and was subjected to sudden cooling effect. The multiple secondary thermal fractures could be created and propagate perpendicular to main fracture with different velocities and final lengths for distinctive temperature difference. This fracture initiation by thermal shock of reservoir rock were demonstrated as well in experiments [8] and analyzed theoretically [9, 10]. The effect of thermal-induced stress on aperture dilation between injection/production wells in long term and instant fracture surface damage by generation of new thermal cracks had also been investigated. They demonstrate the importance of fracture aperture variation on fluid flow and energy extraction by thermal effect. Nevertheless, none of previous studies had paid attention to the instant effect of large thermal stress on integrity of fracture asperities. Appreciable thermal stress due to the rock/water temperature difference would likely damage fracture asperities and result in notable aperture decrease and even the closure of fractures. This study aims to investigate such thermal stress effect on fracture asperity integrity. Through the finite element analysis, the damage of idealized fracture asperity, which is a pair of semi-spheres, due to the rock/water temperature difference has been discussed and demonstrated in this paper.

## 2 Problem Description and Modeling Methodology

Discrete fracture network constitutes the flow paths for fluid in EGS. To simplify the problem and keep focused, one arbitrary fracture is considered without loss of generality. Discrete fracture asperities bolster fracture surfaces and protrude into fluid pathway. Its deformation and integrity are essentially important to fluid transport and heat recovery. Generally, fracture asperities contact with distinct geometries and pairing patterns [11]. To make it tractable, individual asperity is idealized as semi-sphere contact with well mated pattern. Figure 1 depicts the geometry considered in this model at different scales.

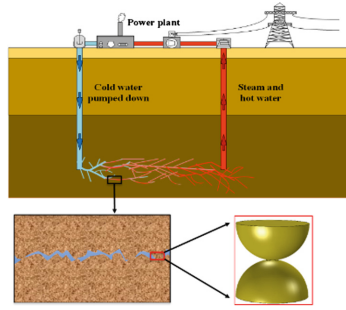


**Fig. 1.** Model geometry at different scales

In this model, both fluid and heat have impact on stress distribution on asperity. The difference of fluid pressure and initial overburden pressure is effective stress loading on asperities. With the exposure to high temperature difference, the fluid pressure change is negligible compared to large thermal stress [12]. Accordingly, the asperity stays at admissible effective stress on top and is subjected to large tensile thermal stress in a short time. Alteration of stress distribution would deteriorate asperity integrity. A quantitative model has been developed to describe the mechanical response of the asperity, which consider both a damage-based constitutive relationship and the temperature field from the heat conduction process.

### 2.1 Constitutive Relations

The constitutive relations for the rock including the thermal strain can be expressed in Eq. (1) [13].

$$\sigma_{ij} = \bar{\lambda}\varepsilon_{kk}\delta_{ij} + \bar{\mu}\varepsilon_{ij} - (3\bar{\lambda} + \bar{\mu})\alpha\Delta T \quad (1)$$

Where  $\sigma_{ij}$  and  $\varepsilon_{ij}$  are the stress and strain tensor, separately.  $\delta_{ij}$  is the Kronecker delta.  $\alpha$  is the coefficient of thermal expansion in material.  $\bar{\lambda}$  and  $\bar{\mu}$  are damage dependent material constants, which follows the form of Lamé's constants and related to damage based elastic modulus,  $\bar{\lambda} = \frac{E\nu}{(1+\nu)(1-2\nu)}$  and  $\bar{\mu} = \frac{E}{2(1+\nu)}$ .  $E$  is the damage

based elastic modulus analyzed in following Eq. (2),  $\nu$  is the Poisson’s ratio. In Eq. (1),  $\epsilon_{ij}$  is sum of mechanical strain and thermal strain in materials,  $\sigma_{ij}$  is the mechanical stress induced only by mechanical strain. This thermal elastic model is suitable for brittle materials with negligible plastic deformation.

The failure of quasi-brittle heterogeneous materials such as rocks is mostly due to propagation and intersection of pre-existing micro-cracks. The micro-cracks connect and eventually form macro-cracks which lead to the failure of the materials [14, 15]. This macroscopic representation of microcrack development can be qualitatively described by continuum damage mechanics [16]. Damage variable is generally introduced to characterize surface density of intersection of micro-cracks in thermodynamic principle [17]. In this study, an isotropic damage variable ( $D$ ) is used to model deterioration of elastic modulus:

$$E = E_0(1 - D) \tag{2}$$

Where  $E$  is the degraded elastic modulus.  $E_0$  is the initial Young’s modulus.  $D$  is an isotropic damage variable,  $0 \leq D \leq 1$ . The value of 0 means element is intact without any modulus degradation. The element loses its loading sustainability and fails when the value is equal to 1.

Referring to laboratory uniaxial experiments of granites [18–20], the uniaxial compression experimental curves has good representation of failure micro-mechanism of granite [21]. Whereas the uniaxial tension loading (usually by indirect Brazilian test) presents distinct features in terms of peak strength and failure modes. In fact, it is the macroscopic realization of different micro-cracking growth and proliferation [22]. In this sense, asymmetric constitutive model is suited for deformation and failure characterization for granites. The constitutive relation is depicted in Fig. 2.

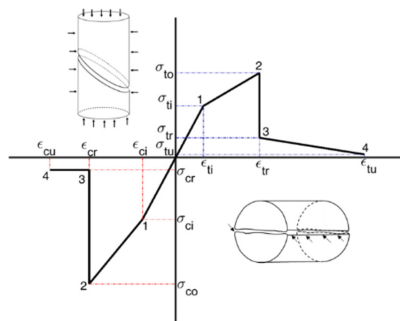


**Fig. 2.** Asymmetric constitutive model for granites and its failure modes under Brazilian test and triaxial compression test.

The definition of the sign in this paper follows that tensile stress is positive and compressive stress is negative. The first quadrant is under tension, while the third quadrant is under compression. The initial stage is elastic deformation. Once the strain threshold (i.e., corresponding to the peak stress) is exceeded, the Young’s modulus will drop dramatically to a small residual value. That indicates the occurrence of element

damage in simulation. A maintenance of small residual value (0.01% of initial value) is needed to avoid computational instability. From Fig. 2, the damage variable for tension and compression can be calculated respectively as:

$$D_t = \begin{cases} 0 & 0 < \varepsilon < \varepsilon_{ti} \\ \left(1 - \frac{\varepsilon_{ti}}{\varepsilon}\right) \left[1 - \frac{\frac{\sigma_{t0}-1}{\varepsilon_{ti}}}{\frac{\sigma_{tr}-1}{\varepsilon_{tr}}}\right] & \varepsilon_{ti} < \varepsilon < \varepsilon_{tr} \\ 1 - \frac{\sigma_{tr}}{\sigma_{ti}} \frac{\varepsilon_{ti}}{\varepsilon} - \frac{\frac{\sigma_{tu}-\sigma_{tr}}{\varepsilon_{ti}}}{\frac{\sigma_{tu}-\sigma_{tr}}{\varepsilon_{tr}}} \left(1 - \frac{\varepsilon_{ti}}{\varepsilon}\right) & \varepsilon_{tr} < \varepsilon < \varepsilon_{tu} \\ 1 & \varepsilon > \varepsilon_{tu} \end{cases} \quad (3)$$

$$D_c = \begin{cases} 0 & \varepsilon_{ci} < \varepsilon < 0 \\ \left(1 - \frac{\varepsilon_{ci}}{\varepsilon}\right) \left[1 - \frac{\frac{\sigma_{c0}-1}{\varepsilon_{ci}}}{\frac{\sigma_{cr}-1}{\varepsilon_{cr}}}\right] & \varepsilon_{cr} < \varepsilon < \varepsilon_{ci} \\ 1 - \frac{\sigma_{cr}}{\sigma_{ci}} \frac{\varepsilon_{ci}}{\varepsilon} & \varepsilon_{cu} < \varepsilon < \varepsilon_{cr} \\ 1 & \varepsilon < \varepsilon_{cu} \end{cases} \quad (4)$$

Where subscript t and c in D is for tension and compression respectively. Other stress and strain parameters signifies stress and strain at inflection points of constitutive curve in Fig. 2.

$$\bar{\sigma} = \begin{cases} |\sigma_1| & \sigma_1 > \sigma_2 > \sigma_3 > 0, \text{ or } \sigma_1 > \sigma_2 > 0 > \sigma_3 \ \& \ \left|\frac{\sigma_1}{\sigma_3}\right| < 0.1 \\ |\sigma_2| & 0 > \sigma_1 > \sigma_2 > \sigma_3, \text{ or } \sigma_1 > 0 > \sigma_2 > \sigma_3 \ \& \ \left|\frac{\sigma_1}{\sigma_3}\right| < 0.1 \end{cases} \quad (5)$$

Where  $\{\sigma_1, \sigma_2, \sigma_3\}$  are three principal stress. In the principal stress system, when material is in tension-tension-tension mode ( $\sigma_1 > \sigma_2 > \sigma_3 > 0$ ) or tension-tension-compression mode ( $\sigma_1 > \sigma_2 > 0 > \sigma_3$ ), the failure is classified to tension failure. While material is subject to compression-compression-compression mode ( $0 > \sigma_1 > \sigma_2 > \sigma_3$ ) or tension-compression-compression mode ( $\sigma_1 > 0 > \sigma_2 > \sigma_3$ ), the failure is classified to compression failure. The restriction  $\left|\frac{\sigma_1}{\sigma_3}\right| < 0.1$  comes from the empirical relationship between compressive and tensile strength of rocks with negligible cohesion forces [23]. Tension failure and compression failure modes can be depicted by failure surface. At here,  $\bar{\sigma}$  is used to depict the failure surface in terms of principal stress.

### 2.2 Temperature Field and Boundary Conditions

The reservoir rock has high initial temperature, denoted as  $T_r$ . When the cold water pumped in with temperature  $T_w$ , rock temperature would drop forward the far field by cooling. This heat transfer follows the Fourier’s Law. Assuming the isotropic thermal property of asperity, the energy balance equation is following:

$$k\nabla^2 T + q = \rho c \frac{\partial T}{\partial t} \quad (6)$$

where  $q$  denotes the heat source generated inside the medium in  $W/m^3$ ,  $k$  is the apparent thermal conductivity of the medium in  $W/m \cdot ^\circ C$ .  $\rho$  is the bulk density of medium in  $kg/m^3$ ,  $c$  is the specific heat or heat capacity of the medium in  $J/kg \cdot ^\circ C$ , and  $t$  is the elapsed time. Equation (6) is on the premise that thermal conductivity  $k$  is constant for temperature change and is a scalar. The top thermal boundary is set to constant temperature  $T_r$ . The curvy surface of hemispherical asperity is set to constant water temperature  $T_w$ . The above assumption is made based on the constant heat source from the adjacent rocks of fracture aperture and the relative small radius of the asperity (radius about 2.5 mm at here) [24]. The parameters in this study is presented as well in Table 1.

**Table 1.** Model data used in simulation

Young's modulus, $E_0$	18.56 GPa	Initial tensile strain, $\varepsilon_{ti}$	$2.2 \times 10^{-4}$
Poisson's ratio, $\nu$	0.25	Residual tensile strain, $\varepsilon_{tr}$	$6.65 \times 10^{-4}$
Granite density, $\rho$	2750 $kg/m^3$	Maximum tensile strain, $\varepsilon_{tu}$	$1.5 \times 10^{-3}$
Heat capacity, $c$	790 $J/kg \cdot K$	Initial tensile stress, $\sigma_{ti}$	4.09 MPa
Thermal conductivity, $k$	10.7 $W/m \cdot K$	Tensile strength, $\sigma_{to}$	6.7 MPa
Thermal expansion, $\alpha$	$8 \times 10^{-6} 1/K$	Residual tensile stress, $\sigma_{tr}$	1.57 MPa
Rock temperature, $T_r$	300 $^\circ C$	Ultimate tensile stress, $\sigma_{tu}$	0.25 MPa
Hemisphere radius, $R$	2.5 mm	Initial compressive strain, $\varepsilon_{ci}$	$2.64 \times 10^{-3}$
Compressive strength, $\sigma_{co}$	100 MPa	Residual compressive strain, $\varepsilon_{cr}$	$6.87 \times 10^{-3}$
Residual compressive stress, $\sigma_{cr}$	9.7 MPa	Maximum compressive strain, $\varepsilon_{cu}$	$1.0 \times 10^{-2}$
		Initial compressive stress, $\sigma_{ci}$	49 MPa

### 3 Results and Discussion

In the deep fracture network of EGS, the asperities are initially subjected to over-burden pressure with initial compressive strain. The overburden pressure increases with the depth of EGS. When cold water is pumped into fracture network, temperature difference between water and rock decreases from the injection well to the production well. Therefore, thermal stress effect on the fracture deformation also varies. Because of the thermal stress, stress on asperities will redistribute, which would lead to asperity deformation and even the damage of asperities. In our study, we took different temperature differences into consideration. Figure 4 shows displacement of asperity subjected to different overburden pressure with and without considering temperature difference effects. It is clear the temperature difference in the EGS could cause considerable asperity deformation. Moreover, different overburden pressure can cause different thermal stress effects. Take  $\Delta T = 50$  K for example (Fig. 3(a)), with the overburden pressure increase, two curves intersect at different points. By considering

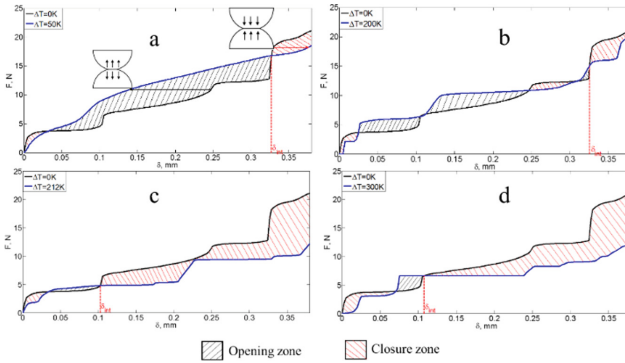


**Fig. 3.** The thermal effect on asperity displacement. With increasing temperature difference, opening zone shrinks and closure zone expands.

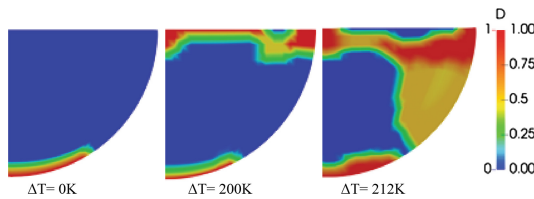


**Fig. 4.** The damaged elements in asperity with increasing temperature.

that the overburden pressure is constant at certain depth in EGS, the introduction of 50 K temperature could induce either the decrease of asperity displacement as indicated by the black arrow in Fig. 3(a) or the increase of asperity displacement as indicated by the red arrow in Fig. 3(a). This means temperature difference can cause either the opening or the closure of fracture. Although it is observed that the closure and opening of fracture occur alternately with varying overburden pressure. Generally speaking, the closure of fracture is more likely to occur for larger overburden pressure. By considering the temperature difference effects, the larger temperature difference can more likely cause the closure of fracture. As mentioned above, the fractures, which are the conduits for water transport and exchange of heat, are critical to the efficiency of EGS. Our results indicate that the temperature difference between water and rock could cause the opening and closure of the fracture, and therefore affect the pre-existing fracture network integrity, which is worthy of more concerns when studying the EGS fracture network.

Figure 4 presents the damage variable for above three temperature difference cases. Because of axisymmetric property of simulating models, only one quarter circle geometry is presented. From evolution of damage variable distribution, more elements damage with increasing temperature difference. Elements near top boundary starts to damage with temperature difference and exacerbate this damage with increasing temperature difference. After  $\Delta T = 200$  K, the damaged elements on top aggregate

together to form a damaged band. However, the influence of temperature difference on evolution of damage at bottom is negligible. This alludes to potential damage on top by temperature effect and potential damage at bottom by displacement closure induced by temperature difference.

## 4 Conclusion

When cold water is pumped into fracture network in enhanced geothermal systems, the huge temperature difference of water and hot rock induces substantial tensile thermal stress. It alters the stress distribution in fracture asperity and changes its deformation. Numerical simulation is employed to capture the effect of temperature difference and intensity of its impact. Damage mechanics considering thermal effect is used in this model to analyze asperity failure. In pure mechanical loading, it presents two modes of deformation: closure and opening. Closure mode jeopardizes integrity of asperity and is of main concern in this analysis. Additionally, with thermal effect, two potential failure mechanisms interplay: (1) bottom failure by mechanical loading; (2) top failure induced by thermal stress. With high temperature difference, top failure becomes significant. High temperature difference also induces closure of asperity and prompts bottom failure. The interplay between these two mechanisms will be analyzed quantitatively. Furthermore, the critical temperature difference to bound closure and opening of asperity is quantified to be 207 K and it's also the boundary to distinguish top failure and bottom failure. In EGS field, zone close to injection well has higher temperature difference and more likely to close and induce asperity failure. While zone close to production well is less prone to damage asperity and more stable. Further analysis will be performed to investigate the relation of asperity failure and flowing length of fluid and reservoir depth.

## References

1. Tester, J.W., Anderson, B.J., Batchelor, A.S., Blackwell, D.D., DiPippo, R., Drake, E., Garnish, J., Livesay, B., Moore, M.C., Nichols, K., Petty, S.: The future of geothermal energy. In: impact of enhanced geothermal systems (EGS) on the United States in the 21st Century, p. 372. Massachusetts Institute of Technology, Cambridge, MA (2006)
2. Bertani, R.: Geothermal power generation in the work 2010–2014 update report. *Geothermics* **60**, 31–43 (2016)
3. Guo, B., Fu, P., Hao, Y., Peters, C.A., Carrigan, C.R.: Thermal drawdown-induced flow channeling in a single fracture in EGS. *Geothermics* **61**, 46–62 (2016)
4. Luo, S., Zhao, Z., Peng, H., Pu, H.: The role of fracture surface roughness in macroscopic fluid flow and heat transfer in fractured rocks. *Int. J. Rock Mech. Min. Sci.* **87**, 29–38 (2016)
5. Pandey, S.N., Chaudhuri, A., Kelkar, S.: A coupled thermo-hydro-mechanical modeling of fracture aperture alteration and reservoir deformation during heat extraction from a geothermal reservoir. *Geothermics* **65**, 17–31 (2017)



6. Bruel, D.: Impact of induced thermal stresses during circulation tests in an engineered fractured geothermal reservoir: example of the Soultz-sous-Forets European hot fractured rock geothermal project, Rhine Graben, France. *Oil Gas Sci. Technol.* **57**(5), 459–470 (2002)
7. Tarasovs, S., Ghassemi, A.: Propagation of a system of cracks under thermal stress. In: 45th US Rock Mechanics/Geomechanics Symposium. American Rock Mechanics Association (2011)
8. Finnie, I., Cooper, G.A., Berlie, J.: Fracture propagation in rock by transient cooling. *Int. J. Rock Mech. Min. Sci. Geomech. Abs.* **16**(1) (1979)
9. Murphy, H.D.: Thermal Stress Cracking and the Enhancement of Heat Extraction From Fractured Geothermal Reservoirs. No. LA-7235-MS. Los Alamos Scientific Lab., N. Mex. (USA) (1978)
10. Barr, D.T.: Thermal Cracking in Nonporous Geothermal Reservoirs. Diss. Massachusetts Institute of Technology (1980)
11. Grasselli, G.: Shear Strength of Rock Joints Based on Quantified Surface Description (2001)
12. Ghassemi, A., Kumar, G.S.: Changes in fracture aperture and fluid pressure due to thermal stress and silica dissolution/precipitation induced by heat extraction from subsurface rocks. *Geothermics* **36**(2), 115–140 (2007)
13. Sadd, M.H.: Elasticity: Theory, Applications, and Numerics. Academic Press, Boston (2009)
14. Ashby, M.F., Sammis, C.G.: The damage mechanics of brittle solids in compression. *Pure. appl. Geophys.* **133**(3), 489–521 (1990)
15. Lockner, D.: The role of acoustic emission in the study of rock fracture. *Int. J. Rock Mech. Min. Sci. Geomech. Abs.* **30**(7) (1993)
16. Tang, C.A., Liu, H., Lee, P.K.K., Tsui, Y., Tham, L.G.: Numerical studies of the influence of microstructure on rock failure in uniaxial compression—part I: effect of heterogeneity. *Int. J. Rock Mech. Min. Sci.* **37**(4), 555–569 (2000)
17. Lemaitre, J.: A continuous damage mechanics model for ductile fracture. *Transactions of the ASME. J. Eng. Mater. Technol.* **107**(1), 83–89 (1985)
18. Okubo, S., Fukui, K.: Complete stress-strain curves for various rock types in uniaxial tension. *Int. J. Rock Mech. Min. Sci. Geomech. Abs.* **33**(6) (1996)
19. Hawkes, I., Malcolm, M., Stephen, G.: Deformation of rocks under uniaxial tension. *Int. J. Rock Mech. Min. Sci. Geomech. Abs.* **10**(6) (1973)
20. Schock, R.N., Louis, H.: Strain behavior of a granite and a graywacke sandstone in tension. *J. Geophys. Res. Solid Earth* **87**(B9), 7817–7823 (1982)
21. Tapponnier, P., Brace, W.F.: Development of stress-induced microcracks in Westerly granite. *Int. J. Rock Mech. Min. Sci. Geomech. Abs.* **13**(4) (1976)
22. Lajtai, E.Z., Bielus, L.P.: Stress corrosion cracking of Lac du Bonnet granite in tension and compression. *Rock Mech. Rock Eng.* **19**(2), 71–87 (1986)
23. Jaeger, J.C., Cook, N.G., Zimmerman, R.: *Fundamentals of Rock Mechanics*. Wiley, New York (2009)
24. Santucci, S., Grob, M., Toussaint, R., Schmittbuhl, J., Hansen, A., Maløy, K.J.: Fracture roughness scaling: A case study on planar cracks. *EPL (Europhysics Letters)* **92**(4), 44001 (2010)